THE JOURNAL OF PHYSICAL CHEMISTRY B

Article

Cite This: J. Phys. Chem. B 2019, 123, 4318−4323

pubs.acs.org/JPCB

Translocation Dynamics of an Asymmetrically Charged Polymer through a Pore under the Influence of Different pH Conditions

Bappa Ghosh and Srabanti Chaudhury*

Department of Chemistry, Indian Institute of Science Education and Research, Dr. Homi Bhabha Road, Pune 411008, Maharashtra, India

Supporting Information

ABSTRACT: We study the translocation of a polymer with oppositely charged segments at both ends of the chain passing through a pore under the effect of an external electric field in the presence of a pH gradient using Langevin dynamics simulations. As observed in experiments, the electrostatic interactions between the pore and the polymer are tuned by altering the pH gradient. Our simulation studies show that with the change in charge distribution on the polymer and the pore that can mimic different pH conditions, the external driving force and the polymer−pore electrostatic interactions play a significant role in the translocation process. The external electric forces are dominant during the entry stage, and the entry time decreases with increase in the charge asymmetry of the pore-trapped polymer. During the exit stage, the electrostatic interactions as well as the external electric field act in concert in determining the exit time through the pore. Our simulation results can capture many features observed in experiments. Our results are explained qualitatively by calculating the free-energy change of the polymer chain during the translocation process.

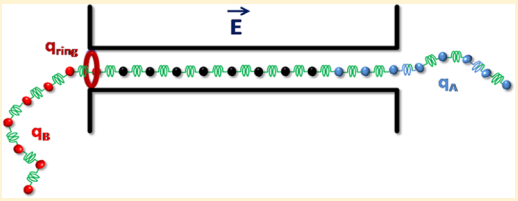

INTRODUCTION

Translocation of polymers through nanometer-sized biological pores and solid-state nanopores has attracted a lot of attention in the last two decades. In a typical experimental setup, a charged polymer is driven across a membrane through an α-hemolysin (α-HL) pore under the influence of an externally applied electric field.[1,2] There are transient blockades in the ionic current when the polymer moves from one side of the nanopore to the other side. Despite a lot of experimental,[1,3] theoretical,[4−7] as well as simulation studies,[8−12] the physics behind this complex translocation process is still elusive. The threading of the polymer chain through the nanopore involves the contribution from the chain entropy, the externally applied electric field, and the polymer−pore interactions. To mention a few, many experiments have been designed to understand the contribution of various factors such as the salt concentration,[13] the sequence of the polymer,[3,14] the applied voltage gradient, the electrostatic interactions,[15] and so on.

A change in the salt concentration gradient or a pH difference can lead to a change in the polymer−pore interaction. It has been shown by Wong and Muthukumar that the charges in the constriction region and at the end of the β-barrel of the pore can be changed by altering the pH.[15] In a recent experimental report by Jeon and Muthukumar,[13] the translocation of a macromolecule from the cis to the trans side of the pore has been studied under various salt concentrations at two different pH conditions (4.5 and 7.5). Their main finding is that the electrostatic interaction between the end of the β-barrel of the pore and the polymer end can be modulated by changing the pH of the solution near the ring region from neutral to more acidic values.[13] Thus, the electrophoretic transport of charged polymers can be controlled by altering the pH gradients across a protein pore. Using all-atom molecular dynamics simulations, it has been shown that the alteration in the pH of the solution has a significant effect on both electroosmotic flow and the anionic selectivity of the pore.[16] The experimental findings were explained theoretically by performing free-energy calculations and calculating the translocation time from the free-energy profile of the polymer.[15,17−20] In a recent study by Ghosh and Chaudhury, extensive molecular dynamics simulations were performed to study the effect of the strength and spatial distribution of charges across a nanopore.[21] This study was motivated by an experimental design where the translocation of a cationic polypeptide was controlled by introducing electrostatic traps at specific regions in the pore lumen.[22] By using a polycationic peptide−peptide nucleic acid probe as the carrier, a nanopore can selectively capture and detect the target miRNA.[23] Also by applying the dielectrophoretic principle, DNA and RNA molecules can be detected selectively by using an engineered biological nanopore.[24] In an experimental study by Luchian and co-workers, it was shown that the capture and transfer of a polypeptide across the nanopore could be controlled by placing oppositely charged amino acid residues at both the chain ends.[25] The experimental results were validated by a simple mathematical model for the free-energy profile along the translocation process and also verified by coarse-grained simulations by considering a polymer with oppositely charged

Received: December 21, 2018
Revised: April 16, 2019
Published: April 16, 2019

DOI: 10.1021/acs.jpcb.8b12301
J. Phys. Chem. B 2019, 123, 4318−4323

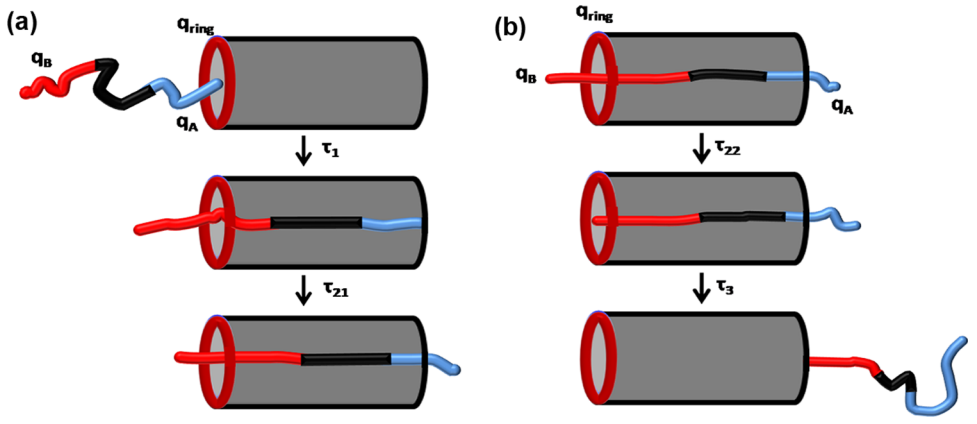

Figure 1. Schematic representation of the 36-bead polymer chain translocation from the trans to the cis side of the pore during (a) entry stage and (b) exit stage. q_A and q_B are the charges on the entry and tail parts of the chain, respectively, and q_{ring} is the charge on the entry side of the pore. For S-I, $q_B = -12e$, $q_{ring} = -7e$; for S-II, $q_B = -4e$, $q_{ring} = 0$; and for S-III, $q_B = -1e$, $q_{ring} = 6e$. $q_A = +12e$ for all of the three systems.

segments at the two ends. As an extension of this work, Luchian and co-workers examined the role of charge asymmetry induced by pH differences in the capture and escape of a peptide containing oppositely charged segments at the N- and C-termini into the α-HL pore and translocating through the nanopore.[26] A pH gradient can alter both the magnitude of charge on the peptide and the pore, thereby controlling the magnitude of peptide−α-HL interactions. The charge asymmetry factor has also been taken into account in a work reported by Chinappi and co-workers, where they proposed a nanopore tweezing approach to study the translocation of asymmetrically and unsymmetrically charged cylindrical rod by adding a positive and a negative tail at the two ends and controlling its residence time by tuning the applied voltage.[27] These experimental techniques have been used to discriminate between neutral amino acid residues from the primary structure of a polypeptide.[28]

In our work, we have performed extensive simulation studies to understand the role of pore−polymer interaction in the translocation of a polymer from trans (β barrel side) to the cis side of the pore where the electrostatic interaction between pore entrance and the two ends of the chain is modulated by altering the trans pH. We consider a coarse-grained picture, and the details about the simulation setup are presented in Model. In Results, we discuss our simulations and explain our numerical results based on the free-energy landscape. Finally, in Conclusions, we summarize our results.

MODEL

The system under study consists of a membrane, a pore, and a charged polymer chain. The polymer chain is composed of $N = 36$ spherical beads each of diameter σ. The excluded volume interactions between beads are modeled by using a short-range repulsive Lennard-Jones (LJ) potential

$$U_{LJ}(r) = 4\epsilon\left[\left(\frac{\sigma}{r}\right)^{12} - \left(\frac{\sigma}{r}\right)^{6}\right] + \epsilon, \quad \text{if } r \le 1.2\sigma \tag{1a}$$

$$U_{LJ}(r) = 0, \quad \text{if } r \ge 1.2\sigma \tag{1b}$$

where r is the distance between two monomer beads, ϵ is the interaction strength, and σ is the diameter of the monomer. The consecutive monomer beads are connected by finitely extensible nonlinear elastic (FENE) springs such that

$$U_{FENE}(r) = -\frac{kR_0^2}{2}\ln\left(1 - \frac{r^2}{R_0^2}\right) \tag{2}$$

where k is the FENE spring constant and R_0 is the maximum allowed separation between consecutive monomers. The wall separating the cis and trans regions is created by LJ particles in the yz plane with the pore oriented along the x axis. To note here, our system of study is not a true polypeptide in the sense that many characteristic features of a polypeptide in terms of folds, torsion angles, and interactions are not taken into account in our current model. In experiments or in vivo condition, the scenario is complicated by atomic charges,[15] electrohydrodynamic interactions,[29,30] electrophoresis,[29,31] protonation−deprotonation due to variation in pH,[31−33] etc. During translocation, most of the time, the polymer remains in extended form. The backbone of the peptide can thus be considered as the single-file motion of the polymer through the pore. Such simple polymer models are well established in previous simulation studies on polymer translocation.[17,21,34,35]

In this work, we consider only the single-file motion of long polymer containing symmetric or asymmetric charged patches at the two ends and a central neutral segment across the pore. In general, the electrostatic interaction between charged particles (polymer−polymer, polymer−pore) is given by the Debye−Hückel screened Coulombic potential

$$U_{coul}(r) = \frac{q_i q_j\, e^{-\kappa r}}{4\pi\epsilon_0 r} \tag{3}$$

where q_i and q_j are charges on beads i and j separated by a distance r. The Debye length $\kappa^{-1} = 0.19$ nm corresponding to a 2 M KCl salt concentration. This small Debye length leads to a strong screening effect,[36] as a result of which the electrostatic interaction among the monomer beads of the polymer chain can be neglected. In our calculations, we only compute the pairwise electrostatic interactions between the pore−polymer beads.

For an α-HL pore that is used as a model system to study translocation, there is a spacious vestibule and the β-barrel connected by a narrow constriction. Wong and Muthukumar estimated the effective charge of the constriction and the ring at the end of the β-barrel as a function of pH.[15] At pH = 7.5, the constriction is neutral while the ring at the mouth of the β-barrel has a charge of $-7e$. On lowering the pH, the pore

DOI: 10.1021/acs.jpcb.8b12301
J. Phys. Chem. B 2019, 123, 4318−4323

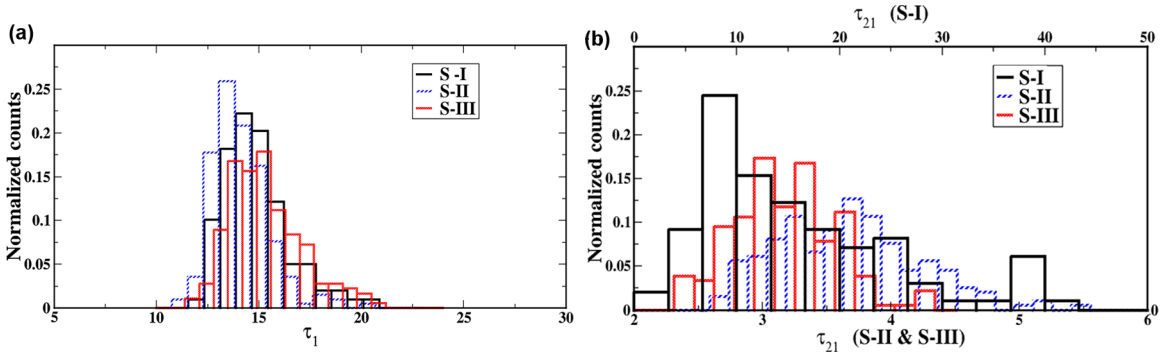

Figure 2. Histogram of translocation time for different systems during the entry stage (a) pore filling, τ_1, (b) the first part of the transfer stage τ_{21} for a chain of length N = 36 and E = 4; the top horizontal axis is for S-I, while the bottom horizontal axis is for S-II and S-III showing different utilized scales.

interior becomes more and more positively charged and the pore becomes more anionic-selective due to the presence of an excess of positive charges on its internal surface.[16,37] The charged state of the constriction and vestibule regions of the α-HL pore is invariant to the change of pH imposed on the trans side of the pore. Due to the high anion selectivity at low pH values, the entry of protons into the pore does not alter the protonation state of the residues located at the constriction or vestibule region. In refs 16 and 26, the charge on the trans entrance of the pore changed with the change in pH, but the charge on the cis entrance and the constriction region remained unaltered. Our model is a simplified case of α-HL pore where the explicit consideration of barrel, constriction, and vestibule regions are not being included. We mainly focus on the cis and trans entrance of a cylindrical pore and the net charge on these regions at different pH gradients. In our simulations, we construct a cylindrical pore composed of 26 consecutive rings of uncharged beads where each ring consists of 16 monomer beads of diameter σ such that the length of the pore is $L = 26\sigma$ and width $W = 3\sigma$. The overall charge on the cis entrance of the pore is taken to be equal to zero at all conditions. In experiments, a pH gradient is created by changing the pH of the trans buffer, thereby altering the net charge on the pore entrance and the charge on the tail part of the polymer added from the trans side. This changes the strength of the electrostatic interactions between the polymer and the pore and also the electrical forces acting on the charged monomers within the pore.[26] The trans pH also induces asymmetry in the charge on the peptide chain. In our simulations, as shown in Figure 1, the charged patch on the first 12 beads is referred to as the A termini and the charged path on the chain end is referred to as B termini. We mimic pH gradients by considering three types of systems as shown in Figure 1. In the first case (S-I), we introduce a positive unit charge on each of the first 12 beads of the chain ($q_A = 12e$, e = 1.60217646 × 10^{-19} C is the elementary charge), the central 12 beads are neutral, and then a unit of negative charge on each of the last 12 beads ($q_B = -12e$). A charge of $-7e$ is distributed among all of the 16 beads that form the first ring of the pore on the entry side (q_{ring}), as shown in Figure 1. This arrangement of charges on the polymer and the pore roughly corresponds to a pH 7.3 on the trans side. In the second and third systems (S-II and S-III, respectively), the charge at the end of the polymer (last 12 monomer beads of the chain) entering the pore from the trans side is changed from $-4e$ to $-1e$ and the charge on the first ring of the pore is changed from $q_{ring} = 0$ to $+6e$ corresponding to roughly pH ∼ 3.7 and ∼3.1.[26] Based on the discussion in the Supporting Information (SI) of ref 26, we assume that for a given system, the charges on the N terminal beads do not change as the chain moves from trans to cis side of the pore.

We simulate the translocation of this partially charged polymer through a nanopore using Langevin dynamics simulations by using the LAMPPS package.[38] In Langevin dynamics simulations, each monomer is subjected to conservative, frictional, and random forces, F_i^C, F_i^F, and F_i^R, respectively.

$$m\ddot{r}_i = -\nabla(U_{LJ} + U_{FENE} + U_{coul}) + F_i^F + F_i^R + F_{ext} \quad (4)$$

where the frictional force F_i^F is given by $F_i^F = -\eta v_i$, v_i is the monomer velocity, η is the friction coefficient, F_i^R is the random force that satisfies the fluctuation−dissipation theorem; and $F_{ext} = q_iE$ is the external force acting parallel to the pore axis on the ith monomer inside the pore due to the presence of an external electrical field, E.

In our simulations, all quantities are expressed in dimensionless LJ unit of energy, length, and mass scales. The time scale is defined as $t_{LJ} = \sqrt{\frac{m\epsilon^2}{\sigma}}$. The dimensionless parameters are $\epsilon_0 = 80$, $\sigma = 1$, $\varepsilon = 1$, $k_BT = 1.2\varepsilon$, $R_0 = 1.5\sigma$, $\xi = \frac{0.7m}{t_{LJ}}$, $k = 30\frac{\epsilon}{\sigma^2}$. With $\varepsilon_{LJ} = 3.39 \times 10^{21}$ J, the temperature T = 300 K. The parameter values used in our simulations are in the range of benchmark parameters reported in previous translocation studies and were effective in explaining experimental results.[17,21,39,40] The scaling of the driving force of the monomer in the pore is $\frac{\epsilon}{\sigma}$, which is about 3.39 pN. In our simulations, the external electric field E is set over a range between 0.1 and 4. This corresponds to the applied voltage of 14−560 mV across the pore. The upper limit of the applied voltage in our simulations is higher than values of applied voltage utilized in typical experiments (30−200 mV). As discussed in the Results section below, to monitor the capture and filling up of the pore in our simulations here, we required a strong electric field to avoid the escape through the trans side.

In general, in the context of polymer translocation, before starting our simulation, the first monomer is placed at the entrance of the pore while the rest of the polymer beads are on the trans side of the pore and then the polymer is allowed to relax to obtain the equilibrium configuration. This constraint is removed and then the whole chain is allowed to evolve according to eq 4 until the chain escapes to the cis side of the

DOI: 10.1021/acs.jpcb.8b12301
J. Phys. Chem. B 2019, 123, 4318−4323

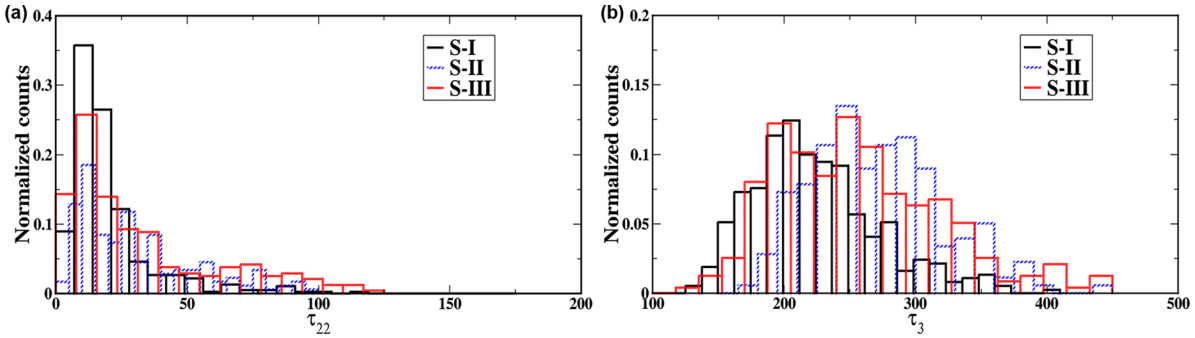

Figure 3. Histogram of translocation time for different systems during the exit stage: (a) the second part of the transfer stage, τ_{22}, (b) pore-emptying stage, τ_3, for a chain of length $N = 36$ and $E = 0.1$.

pore. In a successful translocation event, the translocation[17] time corresponds to the time between the first polymer bead to be just inside the pore at the trans end and the time when the last polymer bead exits the pore on the cis side. The average translocation time is computed from the distribution of translocation times for successful translocations. As described in some previous simulation studies,[21,40] the average translocation time of the polymer τ involves three different time scales: the pore-filling time (τ_1), the transfer time from the trans to cis side of the pore (τ_2), and the pore-emptying time (τ_3). In our current study, τ_2 is further divided into two regimes (τ_{21} and τ_{22}), as shown in Figure 1. The time scale τ_{21} is the time required for the middle bead of the polymer chain to reach the center of the pore. This corresponds to the situation when an equal number of positively and negatively charged monomer beads are arranged symmetrically within the pore. As shown in Figure 1, τ_1 and τ_{21} correspond to the entry stage of the translocation process. We start from this configuration and record the time for the transfer stage (τ_{22}) to be completed. The time scale τ_{22} followed by τ_3 correspond to the exit stage. The integration time step is set to $dt = 0.005$ units. For a given set of parameter values for each system, we perform 200 simulation runs and the histogram of the distributions are constructed from the successful simulation runs using which the average translocation times are obtained. Failed translocation events are rejected and excluded from the statistics. In Figures 2 and 3, the normalized counts on the vertical axis refer to the ratio of the number of successful translocation events in each bin and the total number of successful translocation events. The probability density distributions of the translocation time are normalized to unity.

RESULTS

We consider the translocation of this partially charged polymer chain from the trans to cis side of the pore. To mimic the effect of pH gradients across the pore on the translocation properties, we fix the charge at the cis end of the pore to be zero (corresponding to cis-pH = 7.3) and alter the magnitude of the net charge of the polymer's A-end and the trans end of the pore corresponding to a drop of the trans-pH from 7.3 to 3.17. This allows us to control the sign and the strength of the electrostatic interaction between the charged polymer and the entry side of the pore.

Once the polymer enters the pore, the external electric field drives it from the trans- to the cis-side of the pore. The greater the magnitude of the applied transmembrane potential, the greater the chance of the polymer to fill the pore. For S-I, during the entry stage, the electrostatic attraction between the positively charged beads that have entered the pore and the negatively charged ring at the pore entry ($q_{ring} = -7e$) can slow down the translocation process and the polymer may escape from the trans side itself. To avoid this, the simulations are performed at a strong electric field of $E = 4$, where the electric field effects are significant enough to overcome the electrostatic attractions. For S-II and S-III, the attractive interaction between the A-end moiety and the pore ring decreases and one would expect that the pore to be filled up faster. But as electric field effects dominate and the charge on the end beads that fill up the pore remains invariant for all three systems, in the presence of a strong electric field, the external electric force acting on the monomers inside the pore is the same for all cases. Therefore, there is no significant change in the pore-filling time, as seen in Table 1. Figure 2 shows the translocation time distribution for the polymer chain of length $N = 36$ units for the three different systems that roughly correspond to three different pH gradients.

Table 1. Translocation Times during Entry Stage

E	systems	τ_1	τ_{21}
4.0	S-I	14.78 ± 0.16	15.84 ± 0.98
	S-II	14.08 ± 0.10	3.66 ± 0.04
	S-III	15.34 ± 0.13	3.18 ± 0.03

As shown in Figure 2a, the translocation time distribution for τ_1 is found to have a slightly asymmetric distribution for all the systems. After the pore-filling stage, positively charged residues exit from the cis side and negative residues enter from the trans side of the pore. This gives rise to a charge asymmetry on the pore-trapped chain. Since the charges on the end beads of the polymer decrease for less acidic values, the negative field that pulls back the polymer toward the entrance side is highest for S-I corresponding to a slower translocation and results in a long-tailed distribution, as shown in Figure 2b. For S-II and S-III, the peptide trapped inside the pore is effectively positively charged and is driven to the cis end, thereby making transfer faster, as shown in Table 1, and leads to slightly asymmetric type distribution plots.

During the exit stage, the pore-trapped polymer is becoming more negatively charged. A strong electric field will pull back the monomers toward the trans end, thereby decreasing the probability of a successful translocation event. As a result of this, the simulations during this stage are performed at smaller values of the electric field to prevent escape on the trans side. As shown in Figure 3, we perform simulations to obtain the distributions and calculate the transfer time and pore-emptying

DOI: 10.1021/acs.jpcb.8b12301
J. Phys. Chem. B 2019, 123, 4318−4323

time at $E = 0.1$. For all of the systems, the translocation time distribution for τ_{22} is a long tail distribution, whereas τ_3 shows an asymmetric broad behavior.

For S-I, the electrostatic interaction between the polymer ($q_B = -12e$) and the pore ($q_{ring} = -7e$) is repulsive that facilitates the transfer process. For S-II and S-III, the tail part (B end) of the polymer is less negatively charged and the charge on the pore ring becomes positive, which gives rise to attractive electrostatic interaction, and τ_{22} increases, as shown in Table 2. Based on these arguments, during the escape stage

Table 2. Translocation Times during Exit Stage[a]

E	systems	τ_{22}	τ_3
0.08	S-I	19.54 ± 0.67	192.52 ± 1.94
	S-II	35.77 ± 1.63	215.43 ± 3.23
	S-III	39.91 ± 1.87	209.81 ± 3.18
0.1	S-I	20.30 ± 0.88	203.37 ± 2.39
	S-II	31.11 ± 1.70	241.39 ± 4.12
	S-III	32.42 ± 1.89	224.21 ± 4.29

[a]The values in columns 3 and 4 in the table represent the mean ± standard error of the means for independent successful translocations. The error calculation is shown in the SI.

on the sole basis of the electrostatic interactions, we would expect τ_3 to increase as we go from S-I to S-III. But our simulations show that this trend is not totally followed (Table 2). The escape time for S-III is less than for S-II. The same trend is also observed in the experiments.[26] For S-II and S-III, the pore-captured chain experiences asymmetrical electrical forces acting oppositely on it. This unbalance of the net charge is more for S-III than for S-II. Thus, the pore-captured polymer is more prone to escape from the pore from the cis end for S-III than for S-II. This observed phenomenon could be explained qualitatively from our free-energy calculations. The free-energy E is plotted as a function of the progress variable Q defined as $Q = N_{cis} - N_{trans}$, where N_{cis} and N_{trans} are the number of monomers on the cis and trans sides of the pore, respectively. $N = -35$ corresponds to the beginning of translocation when the first bead is on the trans entrance of the pore and $N = 35$ corresponds to the end of the translocation event when the last bead is on the cis entrance of the pore. The free energy has three contributions: a contribution due to configurational entropy, a contribution due to the electrostatic interaction, and a contribution from the external electric field.[17,26] Following the method used in refs 25 and 26, the free-energy profile can be constructed as a function of the coordinate Q, as shown in the Supporting Information (SI). Figure 4 shows the free-energy landscape for the translocation of a polymer during the pore-emptying stage for S-II and S-III. The asymmetry in the charge distribution on the chain results in a decrease of the free-energy barrier at the cis end during the emptying stage, thereby reducing τ_3 for the latter case.

Similarly, the free-energy landscape for the entry stage can also be constructed and is reported in Figure S1 in the Supporting Information. The free-energy landscape shows that the energy barrier is almost similar for all of the three systems during the pore-filling stage (τ_1) and τ_{21} decreases from I to III, which agrees qualitatively with the trend shown in Table 1. Also as shown in Table 2, for each system, the residence time of the polymer within the pore (τ_3) increases with the increase in the applied electric field. Our simulation results are in qualitative agreement with experiments that show that the

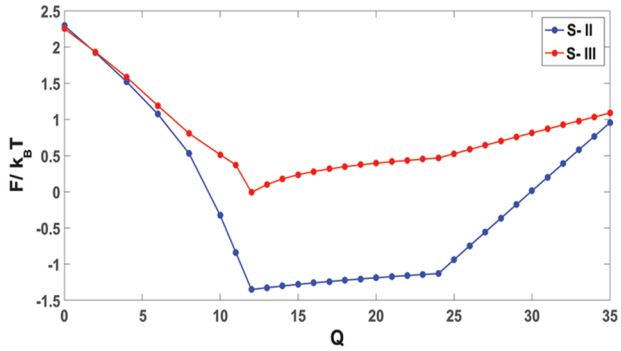

Figure 4. Free-energy landscape for the translocation of a polymer chain of length $N = 36$ during the exit stage (τ_{22} and τ_3) translocating through a pore of length $L = 26$ for S-II and S-III at $E = 0.1$.

residence time of the polymer within the pore increases with the increase in the applied voltage.[26,27]

CONCLUSIONS

In this study, we have performed extensive molecular dynamics simulations to study the effect of polymer−pore interactions on the translocation process by changing the charge distribution of the polymer and the pore to mimic the pH change of the solutions in experimental situations. Experimentally it has been shown that changing the pH alters the charge on the tail part of the polypeptide as well as the charge on the mouth of the β-barrel pore, thereby modulating the electrostatic interactions between the pore and either of the two ends of the peptide. Our simulations show that in the presence of a strong externally applied field, the effect of the electrostatic interactions between the polymer and the pore is minimized during the entry stage of the translocation process. The pore entry time τ_1 is independent of the interactions between the polymer and the pore. During the exit stage of the translocation, the pore-emptying time τ_3 plays a dominant role. In the presence of a weak electric field, the polymer−pore interactions are important and the pore-trapped polymer is expected to be more prone to exit the pore for S-I due to the repulsion between the negatively charged beads at the polymer tail and the negatively charged ring at the pore entrance. At the same time, our simulations show that the unbalanced electric forces acting on both ends of the pore-captured polymer cannot be ignored and play a crucial role in the pore-emptying stage. This is manifested by the fact that the pore-trapped polymer exits the pore faster for S-III than for S-II. Thus, our simulations could capture the dynamics during different stages of the translocation process. The simulation results are also qualitatively supported and explained by free-energy calculations.

ASSOCIATED CONTENT

Supporting Information

The Supporting Information is available free of charge on the ACS Publications website at DOI: 10.1021/acs.jpcb.8b12301.

Estimation of error in the calculation of the mean translocation times, as shown in Tables 1 and 2; calculation of free energy for translocation during entry and exit stages, as shown in Figures 4 and S1 (PDF)

DOI: 10.1021/acs.jpcb.8b12301
J. Phys. Chem. B 2019, 123, 4318−4323

AUTHOR INFORMATION

Corresponding Author

*E-mail: srabanti@iiserpune.ac.in. Phone: 912025908140.

ORCID

Srabanti Chaudhury: 0000-0001-6718-8886

Notes

The authors declare no competing financial interest.

ACKNOWLEDGMENTS

The authors acknowledge DAE-BRNS (37(2)/14/08/2016-BRNS/37022) and IISER Pune for funding. B.G. acknowledges IISER Pune for fellowship. The authors acknowledge Param Yuva C-DAC Pune for computational facilities. They thank Dr. Durba Sengupta, NCL Pune, and Dr. Anup Biswas, IISER Pune, for their valuable suggestions.

REFERENCES

(1) Kasianowicz, J. J.; Brandin, E.; Branton, D.; Deamer, D. W. Characterization of Individual Polynucleotide Molecules Using a Membrane Channel. *Proc. Natl. Acad. Sci. U.S.A.* **1996**, *93*, 13770−13773.

(2) Bezrukov, S. M.; Vodyanoy, I.; Brutyan, R. A.; Kasianowicz, J. J. Dynamics and Free Energy of Polymers Partitioning into a Nanoscale Pore. *Macromolecules* **1996**, *29*, 8517−8522.

(3) Meller, A.; Nivon, L.; Branton, D. P. Voltage-Driven DNA Translocations through a Nanopore. *Phys. Rev. Lett.* **2001**, *86*, 3435.

(4) Sung, W.; Park, P. J. Polymer Translocation through a Pore in a Membrane. *Phys. Rev. Lett.* **1996**, *77*, 783.

(5) Muthukumar, M. Polymer Translocation through a Hole. *J. Chem. Phys.* **1999**, *111*, 10371.

(6) Muthukumar, M. Polymer Escape through a Nanopore. *J. Chem. Phys.* **2003**, *118*, 5174.

(7) Slonkina, E.; Kolomeisky, A. B. Polymer Translocation through a Long Nanopore. *J. Chem. Phys.* **2003**, *118*, 7112.

(8) Luo, K. F.; Ala-Nissila, T.; Ying, S. C. Polymer Translocation through a Nanopore: A Two-Dimensional Monte Carlo Study. *J. Chem. Phys.* **2006**, *124*, No. 034714.

(9) Chuang, J.; Kantor, Y.; Kardar, M. Anomalous Dynamics of Translocation. *Phys. Rev. E* **2001**, *65*, No. 011802.

(10) Vocks, H.; Panja, D.; Barkema, G. T.; Ball, R. C. Pore-Blockade Times for Field-Driven Polymer Translocation. *J. Phys.: Condens. Matter* **2008**, *20*, No. 095224.

(11) Panja, D.; Barkema, G. T.; Ball, R. C. Anomalous Dynamics of Unbiased Polymer Translocation through a Narrow Pore. *J. Phys.: Condens. Matter* **2007**, *19*, No. 432202.

(12) Luo, K.; Huopaniemi, I.; Ala-Nissila, T.; Ying, S. C. Polymer Translocation through a Nanopore under an Applied External Field. *J. Chem. Phys.* **2006**, *124*, No. 114704.

(13) Jeon, B.; Muthukumar, M. Electrostatic Control of Polymer Translocation Speed through α-Hemolysin Protein Pore. *Macromolecules* **2016**, *49*, 9132−9138.

(14) Meller, A.; Nivon, L.; Brandin, E.; Golovchenko, J. A.; Branton, D. Rapid Nanopore Discrimination between Single Polynucleotide Molecules. *Proc. Natl. Acad. Sci. U.S.A.* **2000**, *97*, 1079−1084.

(15) Wong, C. T. A.; Muthukumar, M. Polymer Translocation through α-Hemolysin Pore with Tunable Polymer-Pore Electrostatic Interaction. *J. Chem. Phys.* **2010**, *133*, No. 045101.

(16) Bonome, E. L.; Cecconi, F.; Chinappi, M. Electroosmotic Flow through an α-Hemolysin Nanopore. *Microfluid. Nanofluid.* **2017**, *21*, No. 96.

(17) Katkar, H. H.; Muthukumar, M. Effect of Charge Patterns Along a Solid-State Nanopore on Polyelectrolyte Translocation. *J. Chem. Phys.* **2014**, *140*, No. 135102.

(18) Sun, L. Z.; Cao, W. P.; Luo, M. B. Free Energy Landscape for the Translocation of Polymer through an Interacting Pore. *J. Chem. Phys.* **2009**, *131*, No. 194904.

(19) Chen, Y.-C.; Wang, C.; Zhou, Y. L.; Luo, M.-B. Effect of Attractive Polymer-Pore Interactions on Translocation Dynamics. *J. Chem. Phys.* **2009**, *130*, No. 054902.

(20) Zhang, S.; Wang, C.; Sun, L.-Z.; Li, C.-Y.; Luo, M.-B. Polymer Translocation through a Gradient Channel. *J. Chem. Phys.* **2013**, *139*, No. 044902.

(21) Ghosh, B.; Chaudhury, S. Influence of the Location of Attractive Polymer−Pore Interactions on Translocation Dynamics. *J. Phys. Chem. B* **2018**, *122*, 360−368.

(22) Mohammad, M. M.; Prakash, S.; Matouschek, A.; Movileanu, L. Controlling a Single Protein in a Nanopore through Electrostatic Traps. *J. Am. Chem. Soc.* **2008**, *130*, 4081−4088.

(23) Tian, K.; He, Z.; Wang, Y.; Chen, S.-J.; Gu, L.-Q. Designing a Polycationic Probe for Simultaneous Enrichment and Detection of MicroRNAs in a Nanopore. *ACS Nano* **2013**, *7*, 3962−3969.

(24) Tian, K.; Decker, K.; Aksimentiev, A.; Gu, L. Q. Interference-Free Detection of Genetic Biomarkers Using Synthetic Dipole-Facilitated Nanopore Dielectrophoresis. *ACS Nano* **2017**, *11*, 1204−1213.

(25) Asandei, A.; Chinappi, M.; Lee, J.-k.; Seo, C. H.; Mereuta, L.; Park, Y.; Luchian, T. Placement of Oppositely Charged Aminoacids at a Polypeptide Termini Determines the Voltage-Controlled Braking of Polymer Transport through Nanometer-Scale Pores. *Sci. Rep.* **2015**, *5*, No. 10419.

(26) Asandei, A.; Chinappi, M.; Kang, H.-K.; Chang, H. S.; Mereuta, L.; Park, Y.; Luchian, T. Acidity-Mediated, Electrostatic Tuning of Asymmetrically Charged Peptides Interactions with Protein Nanopores. *ACS Appl. Mater. Interfaces* **2015**, *7*, 16706−16714.

(27) Chinappi, M.; Luchian, T.; Cecconi, F. Nanopore Tweezers: Voltage-Controlled Trapping and Releasing of Analytes. *Phys. Rev. E* **2015**, *92*, No. 032714.

(28) Asandei, A.; Rossini, E.; Chinappi, M.; Park, Y.; Luchian, T. Protein Nanopore-Based Discrimination between Selected Neutral Amino Acids from Polypeptides. *Langmuir* **2017**, *33*, 14451−14459.

(29) Luan, B.; Aksimentiev, A. Electric and Electrophoretic Inversion of the DNA Charge in Multivalent Electrolytes. *Soft Matter* **2010**, *6*, 243−246.

(30) Ghosal, S. Effect of Salt Concentration on the Electrophoretic Speed of a Polyelectrolyte through a Nanopore. *Phys. Rev. Lett.* **2007**, *98*, No. 238104.

(31) Buyukdagli, S.; Ala-Nissila, T. Ph-Mediated Regulation of Polymer Transport through Sin Pores. *EPL* **2018**, *123*, No. 38003.

(32) Buyukdagli, S.; Ala-Nissila, T. Controlling Polymer Translocation and Ion Transport Via Charge Correlations. *Langmuir* **2014**, *30*, 12907−12915.

(33) Buyukdagli, S.; Ala-Nissila, T. Controlling Polymer Capture and Translocation by Electrostatic Polymer-Pore Interactions. *J. Chem. Phys.* **2017**, *147*, No. 114904.

(34) Hsiao, P.-Y. Polyelectrolyte Threading through a Nanopore. *Polymers* **2016**, *8*, No. 73.

(35) Sarabadani, J.; Ikonen, T.; Ala-Nissila, T. Iso-Flux Tension Propagation Theory of Driven Polymer Translocation: The Role of Initial Configurations. *J. Chem. Phys.* **2014**, *141*, No. 214907.

(36) Oukhaled, G.; Bacri, L.; Mathe, J.; Pelta, J.; Auvray, L. Effect of Screening on the Transport of Polyelectrolytes through Nanopores. *EPL* **2008**, *82*, No. 48003.

(37) Aksimentiev, A.; Schulten, K. Imaging α-Hemolysin with Molecular Dynamics: Ionic Conductance, Osmotic Permeability, and the Electrostatic Potential Map. *Biophys. J.* **2005**, *88*, 3745−3761.

(38) Plimpton, S. Fast Parallel Algorithms for Short-Range Molecular Dynamics. *J. Comput. Phys.* **1995**, *117*, 1−19.

(39) Sarabadani, J.; Ghosh, B.; Chaudhury, S.; Ala-Nissila, T. Dynamics of End-Pulled Polymer Translocation through a Nanopore. *EPL* **2017**, *120*, No. 38004.

(40) Luo, K.; Ala-Nissila, T.; Ying, S. C.; Bhattacharya, A. Influence of Polymer-Pore Interactions on Translocation. *Phys. Rev. Lett.* **2007**, *99*, No. 148102.

DOI: 10.1021/acs.jpcb.8b12301
J. Phys. Chem. B 2019, 123, 4318−4323